MODELING AND FUZZY LOGIC CONTROLLER DESIGN FOR LABORATORY SCALE 3DOF UOTCS HELICOPTER

Prof Dr. Waladin K. Said * **Mothena Fakhri Shaker ***

Received on: 14/9/2008
Accepted on: 21/7/2009

Abstract

The UOTCS (*U*niversity *O*f *T*echnology *C*ontrol *S*ystem) helicopter system is a laboratory scale experimental platform developed primarily for teaching system dynamics and control engineering principles to undergraduate students. It also provides an excellent research platform for control and mechatronics postgraduate students. This paper is concerned with the modeling and controllers design for the UOTCS helicopter to mimics its motion. The kinematics model was derived following the Denavit-Hartenberg theory while the dynamic model was based on Euler-Lagrange equations of motion. The helicopter mathematical model includes the inertias of the counterweight, the beams and the propeller motors. This model was found competent enough for this application as it describes the dominant behaviors and coupling among the degrees of freedom of the helicopter model. Fuzzy logic controllers for elevation and pitch motion control were designed. The performance of the FLC is compared with the classical PID controller and the results are evaluated. Fuzzy logic controllers are suitable to control the elevation and pitch motions of the UOTCS helicopter.

Keywords: Helicopter modeling, Simulation, Fuzzy Logic Control, Teaching platform.

نمذجة و تصميم مسيطر منطق مضبب لمنظومة مروحية أل (UOTCS) ذي ثلاث درجات حرية المختبرية

الخلاصة

يُقدم البحث تمثيل وتصميم مسيطر للمروحية (UOTCS) و التي صُنعت في قسم هندسة السيطرة و النظم في الجامعة التكنولوجية. قد طُورت هذه المروحية ابتداءً لتعليم ديناميكية ألانظمه وأساسيات هندسة السيطرة لطلبة الدراسات الأولية. كذلك فان المنظومة تُوفر منصة بحث ممتازة لطلبة الدراسات العليا في هندسة السيطرة والميكاترونيكس. طُور النموذج الرياضي لكي يشابه حركة المروحية (UOTCS). وقد اشتُق النموذج الكُينماتيكي بإِتباع نظرية (Denavit-Hartenberg) بينما اعتمد النموذج الديناميكي على معادلات (Euler-Lagrange) للحركة. يشمل النموذج الرياضي عزم القصور الذاتي لكل من كتلة الموازنة و الحاملات ومحركي المروحيتين. وُجد النموذج الرياضي ملائماً للتطبيق حيث يصف السلوكيات المؤثرة والتعشيق بين درجات الحرية لنموذج المروحية. كذلك يقدم البحث تصميم مسُيطرات منطقية ضبابية لكل من حركة الارتفاع و الميل لمروحية ال(UOTCS). قُورن أداء مسيطر المنطق المضبب مع المسيطر التقليدي (PID) و تشير النتائج الى أن أداء المسيطرات المنطقية الضبابية جيدة و مناسبة للسيطرة على حركتي الارتفاع والميل (elevation and pitch) لمروحية (UOTCS).وظُفت الصياغات الواقعية الحقيقية لإحياء وإظهار نتائج المحاكاة صوريا.حيث استُعملت لغة النموذج الواقعي الحقيقي لخلق نموذج مروحية ثلاثية الأبعاد.

* Control and Systems Eng. Dept., UOT. Baghdad, Iraq.

1. Introduction

Hardware-in-the-loop (HIL) simulation is an approach to shorten new product development cycle. Helicopter laboratory processes is a typical example of HIL simulation. The UOTCS (the abbreviation stands for *U*niversity *O*f *T*echnology *C*ontrol *S*ystem) helicopter system is an experimental platform manufactured at the department of Control and Systems Engineering / University of Technology. This system has been a part of a laboratory facility provided by the CS Dept. since 2007 [1]. It presents a useful experimental platform for advanced students and researchers in the field of control and mechatronics to practice their skills in modeling, system identification, robust control and real time software design [2]. Such a setup is a MIMO type with nonlinear dynamics and static input nonlinearities. It may prove helpful for nonlinear controller design and identification of a linear model.

The UOTCS helicopter is mounted on a table top and its primary components are the main beam, the twin rotor assembly and the counterweight, as shown in figure (1). The rotational motion about the vertical axis is called (travel). It occurs about a vertical axis which goes through the slip–ring and is perpendicular to the table. The main beam can be raised and lowered about a horizontal pivot. This motion is called (elevation) and it occurs about an axis which goes through the slip–ring assembly and is parallel to the table. At one end of the main beam, there is another bearing whose axis is collinear with the beam's axis. It allows a set of twin rotors driven by DC motors to pivot around that bearing. The resulting motion is called (pitch). The pitch motion of the rotors gives rise to the travel motion of the assembly. At the other end of the main beam, there is a counterweight which reduces the power requirements on the motors by reducing the effective weight of the rotor assembly in the horizontal position [1, 3].

The UOTCS helicopter is a complex system having high nonlinearity and coupling among its degrees of freedom. The goal of this research is to upgrade the helicopter mathematical model that was developed in reference [1] to include the inertias of the counterweight, the beams and the motors. Further more, to design fuzzy logic pitch and elevation controllers and asses their performance. The ultimate objective is to provide a safe educational laboratory apparatus that satisfies laboratory experience for the students in the fields of system dynamics, parameter identification, and nonlinear control theory. The provision of a UOTCS helicopter animation using virtual reality is an additional useful tool for teaching control students.

Mathematical modeling of the UOTCS helicopter will be explained next in section 2. Section 3 discusses elevation and pitch controllers design.

2. Modeling

The UOTCS helicopter mathematical model was obtained by applying kinematics analysis first and then the dynamic equations of motion of the system is derived. Figure (2) shows the coordinate system assignment of the UOTCS helicopter using the Denavit–Hartenberg (D-H) convention [4]. The right-hand Cartesian world coordinate system, $O_0(x_0y_0z_0)$, is established at the intersection of the main bearings and the slip-ring assembly. The seven coordinate systems $O_1(x_1y_1z_1)$, $O_2(x_2y_2z_2)$ .. to $O_7(x_7y_7z_7)$, are setup as shown in figure (2). The origins of the first and second coordinates coincide with that of the world system. Table (1) defines the link parameters a_i, α_i, d_i, and θ_i based on the D-H convention, where i = 1, 2,…….7 [4].

The overall transformation between any two desired points is obtained by consecutively multiplying the homogeneous transformation matrices $\boldsymbol{T}_i$ between axes *i* and *i-1* (reference [5]) for all axes in between. For example, the forward kinematics, from base to counterweight ($\boldsymbol{T}_c$) is given by multiplying the homogeneous transformation matrices $\boldsymbol{T}_1$ (from O_0 to O_1) and $\boldsymbol{T}_7$ (from O_1 to O_7), i.e;

$$\boldsymbol{T}_c = \begin{bmatrix} -C_\lambda C_\varepsilon & -S_\lambda & -C_\lambda S_\varepsilon & -L_w C_\lambda C_\varepsilon \\ -S_\lambda C_\varepsilon & -C_\lambda & -S_\lambda C_\varepsilon & -L_w S_\lambda C_\varepsilon \\ -S_\varepsilon & 0 & 0 & -L_w S_\varepsilon \\ 0 & 0 & 0 & 1 \end{bmatrix} \quad ….(1)$$

Where S and C are used to designate sine and cosine of the angle, respectively. Similarly, the forward kinematics of the back motor (figure (2)) is obtained by multiplying the homogeneous transformation matrices $\boldsymbol{T}_1$ (from O_0 to O_1), $\boldsymbol{T}_2$ (from O_1 to O_2), $\boldsymbol{T}_4$ (from O_2 to O_4) and $\boldsymbol{T}_6$ (from O_4 to O_6). The resulting transformation and other transformations can be found in reference [6].

By using Euler-Lagrange's equations of motion of the system, a set of differential equations describing the motion of the UOTCS helicopter in terms of its joint variables and its structural parameters were derived [6]. The derivation is based on the kinetic and potential energies of the entire system; it is expressed by [4];

$$\frac{\mathrm{d}}{\mathrm{d}t}\frac{\partial \boldsymbol{L}}{\partial \dot{\boldsymbol{q}}}-\frac{\partial \boldsymbol{L}}{\partial \boldsymbol{q}}=\boldsymbol{Q} \qquad \text{..... (2)}$$

where, $\boldsymbol{L}$ is the Lagrangian and it represents the difference between the Kinetic and Potential energies of the system. Also, $\boldsymbol{q} = [\boldsymbol{q}_1, \boldsymbol{q}_2,\ldots..\boldsymbol{q}_n]^{\mathrm{T}}$ is the set of generalized coordinate for the system and $\boldsymbol{Q} = [\boldsymbol{Q}_1, \boldsymbol{Q}_2,\ldots..\boldsymbol{Q}_n]^{\mathrm{T}}$ is the vector of generalized forces acting on the system. In order to simplify and derive the final form of the equations several assumptions are made, they are;

- The propellers are rigid and have no twist.
- The simulator structure is rigid and symmetrical therefore the main beam does not create any moments.
- The effects of friction of the joints and those of the slip rings and brushes are negligible.

To solve equation (2), the Jacobian matrix, $\boldsymbol{J}$, of the UOTCS helicopter was determined first. $\boldsymbol{J}$ is a $6\times$n matrix consisting of $[\boldsymbol{J}_v\ \boldsymbol{J}_\omega]^{\mathrm{T}}$, where the upper part, $\boldsymbol{J}_v$, and the lower part, $\boldsymbol{J}_\omega$, are the linear and angular velocity Jacobian matrices, respectively. The resulting equation of motion of the helicopter model expressed in matrix form is obtained in the form [4];

$$\boldsymbol{D}(\boldsymbol{q})\,\ddot{\boldsymbol{q}} + \boldsymbol{C}(\boldsymbol{q},\dot{\boldsymbol{q}})\,\dot{\boldsymbol{q}} + \boldsymbol{g}(\boldsymbol{q}) = \boldsymbol{\tau} \quad \text{........(3)}$$

Where $\boldsymbol{D}(\boldsymbol{q})$ is a symmetric positive matrix which is in general configuration dependent and it is called inertia matrix. The overall inertia matrix $\boldsymbol{D}(\boldsymbol{q})$ of the UOTCS helicopter was determined by adding the inertia matrices of the counterweight $(\boldsymbol{D}(\boldsymbol{q})_c)$, main beam $(\boldsymbol{D}(\boldsymbol{q})_a)$, front motor $(\boldsymbol{D}(\boldsymbol{q})_f)$, back motor $(\boldsymbol{D}(\boldsymbol{q})_b)$ and pendulum link $(\boldsymbol{D}(\boldsymbol{q})_h)$; that is [1];

$$\boldsymbol{D}(\boldsymbol{q}) = \boldsymbol{D}(\boldsymbol{q})_c + \boldsymbol{D}(\boldsymbol{q})_a + \boldsymbol{D}(\boldsymbol{q})_f + \boldsymbol{D}(\boldsymbol{q})_b + \boldsymbol{D}(\boldsymbol{q})_h \quad \text{.......(4)}$$

In equation (3), the elements of the matrix $\boldsymbol{C}(\boldsymbol{q},\dot{\boldsymbol{q}})$ were calculated by using the Christoffel symbols [4, 6].

The torque term $\boldsymbol{g}(\boldsymbol{q})$ in equation (3) is due to gravitational forces. It is simply the mass multiplied by the gravitational acceleration and the height of the center of each mass. These are the centre of mass of the counterweight, front and back motors, the main beam and the pendulum-link.

Finally, the last term is the torque matrix. It was be calculated by using [5];

$$\boldsymbol{\tau} = \boldsymbol{J}(\boldsymbol{q})^{\mathrm{T}}\,\boldsymbol{F} \quad \text{.....(5)}$$

Where, $\boldsymbol{F}$ is the force vector. In other words the forces F_f, F_b of the front and back motors are related to the joint torques by the transpose of the system Jacobian matrix. The relationship between the generalized joint torque $\boldsymbol{\tau}(\boldsymbol{q})$ vector and the external generalized force $\boldsymbol{F}$ exerted by the (n) links on the environment in a specific configuration is;

$$\boldsymbol{\tau}(\boldsymbol{q}) = \boldsymbol{J}_{nv}^{\mathrm{T}}\,\boldsymbol{F} \quad \text{......(6)}$$

Where $\boldsymbol{J}_{nv}^{\mathrm{T}}$ is the transpose Jacobian matrix $\boldsymbol{J}_v$, linear velocity Jacobian, of n links. The entries of the Jacobian matrix depend on the values of the joint variables, and they are usually expressed relative to the base coordinate system. Therefore, the components of the external generalized force vector $\boldsymbol{F}=[F_x\ F_y\ F_z]^{\mathrm{T}}$ must also be expressed relative to the base coordinates. Thus F_x, F_y, F_z are the components of the force at the ends. As shown in figure (2) the 3DOF UOTCS helicopter has two external forces F_f and F_b acting at two points O_5 and O_6, respectively. The F_f and F_b are the forces produced by the Front and Back propellers, respectively. The generalized force vector $\boldsymbol{F}$ for this configuration can be represented as;

$$\boldsymbol{F}_0^{front} = \boldsymbol{R}_0^5\,.[0\ \ 0\ \ F_f\,]^{\mathrm{T}}$$
$$\boldsymbol{F}_0^{back} = \boldsymbol{R}_0^6\,.[0\ \ 0\ \ F_b\,]^{\mathrm{T}} \quad \text{... (7)}$$

2.1 Simulation:

The kinematics and dynamic equations of the UOTCS helicopter were programmed using MATLAB software. Various MATLAB files and functions were built for this purpose. The output of these files and functions is a general nonlinear model presented in a symbolic form. A simulink block named MATLAB Fnc (MATLAB Function) which contains a script MATLAB function dedicated to solving the model's nonlinear differential equation was built. A simulink nonlinear model of the UOTCS helicopter was implemented, as shown in figure (3a). The interested reader may refer to references [1, 6] for further details.

Figure (3a) shows that the inputs are the helicopter system parameters (*Length block*: L_{af}, L_c, L_w, L_h; *Mass block*: m_p, m_c, m_a, m_h; *Inertia block*: I_{xc}, I_{zc}, I_{xp}, I_{zp}, I_{xa}, I_{ya}, I_{za}, I_{xh}, I_{yh} and I_{zh}), control inputs (F_f and F_b), angular positions and velocities. MATLAB Fnc outputs are the angular accelerations $\ddot{\boldsymbol{q}}$. The latter vector is fed to a subsystem block named "angles" to integrate it twice to generate $\dot{\boldsymbol{q}}$ and $\boldsymbol{q}$ vectors.

The initial values of $\boldsymbol{q}$ and $\dot{\boldsymbol{q}}$ can be easily added to the integral blocks as required by the operator. However, for any initial ε, L_w should be adjusted for a given F_f and F_b or vice-versa. Using equation (2), it can be shown that for any $\boldsymbol{q}$ and $\dot{\boldsymbol{q}} = \ddot{\boldsymbol{q}} = 0$ [6];

$$L_w = [h(2m_p + m_h)tan(\varepsilon) + 2m_p L_{af} + m_h L_{af} + m_a L_c - L_{af}(F_f + F_b)/gcos(\varepsilon)]/m_c \quad ..(8)$$

Equation (8) relates the length L_w to the elevation angle (ε) at the equilibrium point with zero pitch angle.

2.2 Linearization

The provision of a linearized model about an arbitrary equilibrium operating point is crucial to make the necessary requirements available for the FLC design. Linearization is accomplished by determining the variation equations about an equilibrium point using Taylor series expansion technique. A numerical equivalent linear system was developed for the UOTCS helicopter at any desired operating point expressed in the form [6];

$$\dot{\boldsymbol{x}}(t) = \boldsymbol{A}\,\boldsymbol{x}(t) + \boldsymbol{B}\,\boldsymbol{u}(t) \quad ....(9)$$

Where, $\boldsymbol{x}(t) = [\lambda, \varepsilon, \theta, \dot{\lambda}, \dot{\varepsilon}, \dot{\theta}]^T$ and $\boldsymbol{u}(t) = [F_f, F_b]^T$ represent variation of the state from an operating point. Matrices $\boldsymbol{A}$ and $\boldsymbol{B}$ are functions of the states and inputs for each operating point. Table (2) summarizes a number of elevation and pitch motions transfer functions obtained for an arbitrarily selected operating points. The table shows a variation of about 30% and 20% in elevation and pitch time constants, respectively. Also, the elevation gain exhibited a 33% change.

3. FLC Controller Design

Elevation and pitch motion fuzzy logic controllers were designed. Each controller has two inputs and one output. Figure (4) shows the elevation controller schematically. The pitch controller is similar to that shown in figure (4) except that the gains k_{e1}, k_{e2}, k_{oe} are replaced in respective order by k_{p1}, k_{p2}, k_{op}. The input and output universes of the fuzzy controllers are normalized in the range (-1, 1). The gains k_{e1}, k_{e2}, k_{p1} and k_{p2} are used to map the actual inputs of the fuzzy system to the normalized universes of discourse (-1, 1) and are called normalizing gains. Similarly k_{oe} and k_{op} are the output gains that scale the output of the controllers.

The elevation and pitch controllers use triangular membership functions. The membership functions for the input fuzzy sets are uniform and similar for the elevation and pitch controllers. Figure (5a) shows the elevation controller membership functions. The membership functions for the output fuzzy sets are narrower near zero for elevation and pitch controllers (figure (5b)). This serves to decrease the gain of the controller near the set point so a better steady state control can be obtained and yet avoid excessive overshoot [7]. The output membership function for the elevation controller is similar to that of the pitch controller (shown in figure (5b)) but has equally spaced center values for the membership function, i.e., PS, PM and PB assume the values ⅓, ⅔ and 1.

The rule base array that was used for elevation and pitch controllers is the same. Each rule base is a 7×7 array, since there are 7 fuzzy sets on the input universes of discourse, as shown in table (3).The topmost rows show the indices for the seven fuzzy sets of the derivative for the position error input e, and the column at the extreme left shows the indices for the seven fuzzy sets for the position error input. The body of the table shows the indices action for input in Fuzzy implications of the form:

IF premise **THEN** consequent.

For example: **IF** error is negligible **and** change-in-error is positive-small **THEN** output is positive-small.

To design the controllers, the normalized gains k_{e1}, k_{e2} and k_{oe} for the elevation controller were tuned by trial and error to obtain minimum overshoot and steady state error response to unit step inputs in elevation angle using the linearized models of table (2). Figure (6) shows the response (continuous curves) where the transfer function for the operating point $\boldsymbol{q}$=[0 -30 0]^T and $\dot{\boldsymbol{q}}=\mathbf{0}$ was used. The values of k_{e1}, k_{e2} and k_{oe} thus obtained are 0.3, 0.07 and 15, respectively. The same design producer was followed for the pitch fuzzy logic controller. The controller parameters k_{p1}, k_{p2} and k_{op} were found to be 0.46, 0.04 and 17, respectively. Dotted curves of figure (6) show pitch angle responses to unit step inputs.

3.1 <u>FLC for the UOTCS Helicopter</u>

A nonlinear simulator for the UOTCS helicopter with elevation and pitch motion controllers was implemented in simulink, as shown in figure (3b). The saturation nonlinearities are used to put limits on the propeller thrust force with zero lower limits. A series of numerical tests were carried out using the nonlinear simulator to tune up the linearized system based FLC parameters. Figures (7a) and (7b) show typical pitch (-5^o) step and elevation (from -10^o to 30^o) responses after tuning. The new elevation controller gains k_{e1}, k_{e2} and k_{oe} are 0.5, 0.64 and 18, respectively. The pitch controller gains remained the same as those obtained with the linearized model.

Two main groups of numerical tests were carried out to test the controllers and asses the degree of coupling between the helicopters' inputs and outputs. For the first group, the initial elevation of the UOTCS helicopter was -15˚ with *zero thrust force* and subjected to either a step change in elevation and/or pitch inputs. The necessary counterweight position L_w setting was 0.2235 m in order to maintain the elevation at -15˚. The final position for this group of tests is 20˚. Group two of the tests are similar to those of group one except for the initial conditions. An *initial thrust force* was applied to maintain level initial position. This represents the case when the helicopter was loaded and it was just about to take off.

Figure (8) shows elevation angle responses (curves set (a)) to step inputs from -15˚ to 20˚ position. Curve (a1) is the response of the nonlinear model with thrust force saturation and gain ½. No change in response is obtained when the gain is increased to unity (curve (a2)). Curve (a3) shows the response of the nonlinear model without thrust force saturation. A comparison with curve (a4) shows that there is a minor change in response with negligible steady state error. Figure (8) also shows the elevation responses under conditions of simultaneous step inputs in elevation and pitch (curves set (b)). Using thrust force saturation with half and unity gains, the responses of curves (b1) and (b2)) are obtained in respective order. The pitching maneuver affects elevation movement only when there is saturation in the thrust force. The peak overshoot has increased to 28.5% for curve (b1) and 30% for curve (b2). Following the same order of systems, the settling time has increased from 8.5 to 11 seconds. Curves (b3) and (b4) in figure (8) reflect the coupling is rather weak when there is no saturation. In conclusion, the pitching motion affects elevation motion only when there is saturation in the thrust force. The pitch angle responses shown in figure (9) show a similar tendency in its behaviour.

Figure (10) is a sample of representative results for group two of the numerical tests, where the same trend in behavior is exhibited.

3.2 Discussion of Controllers Performance

To evaluate helicopter's elevation and pitch maneuvering quality with FLCs, its performance is compared with PID controllers. Using the UOTCS helicopter nonlinear simulator, a series of numerical tests were carried out and figures (11) to (16) summarize typical simulation results. In all these tests, the masses and moments of inertias of the main beam and pendulum link together with the mass moment of inertias of the counterweight, front and back motors are taken into account. In some figures; namely; figures (13), (15) and (16), this model is referred to as the first model. The second model reported in figures (13), (15) and (16) refers to the model used in reference [1] where the masses and moments of inertias of the main beam and pendulum link were assumed zero. The operating point of the UOTCS helicopter considered for all these tests are -30˚ elevation with zero thrust force.

Figure (11) shows elevation angle responses to a step input from –30º to 0º position. Curve (a1) is the UOTCS response using FLC with thrust force saturation. There is no peak overshoot and the output reach level position in 8 seconds. The response is not seriously influenced by the controller gain (curve (a2)). When using the PID controller the peak overshoot increases to (25.8%) and the settling time increases to 10 seconds (curves (b1) and (a1)). Curve (a3) shows the response of the helicopter with FLC without thrust force saturation. Again, no peak overshoot is shown and the settling time is 8 seconds. The corresponding PID controller response (curve (b3)) shows a peak overshoot of (8.3%) with 9.5 seconds settling time.

Figure (12) presents a performance comparison of FLC, PID and PD pitch controllers for pitch only maneuver. The performance with PID and PD controllers is sensitive to the saturation nonlinearity as indicated by curves (b1) and (b3) (for gains ½ and 1) or (b2) and (b4). Using the PD pitch controller leads to steady state error as shown by curves (b1) and (b3). Curves (a1) and (a2) clearly point out the robustness of the FLC to saturation nonlinearity and its fast response.

The performance of the FLCs under conditions of coupling between elevation and pitch motions is shown in figure (13). Simultaneous step inputs are applied to both inputs (elevation (-30^o to 0^0) and pitch (0^o to -5^o)) with and without saturation thrust forces. The corresponding UOTCS responses with PID controllers are also shown (continuous curves). The FLC shows a peak overshoot of 33% and settling time 9.5 seconds (curve (a1)) as compared with 53% and 13.5 seconds when PID controller is used (curve (b1)). When a PD pitch motion controller is used, the peak overshoot is reduced to 37% and the settling time to 11 seconds, as shown by curve (b1) in figure (14). Figure (15) shows the pitch angle response. The steady state error is a result of the PD action. The figure clearly displays the same trend of the superiority of the FLC in terms of robustness and speed of response.

The dotted curves shown in figures (13), (15) and (16) are obtained when the second model is used, where the inertias of the propeller motors, counterweight and beams are assumed negligible as reported in reference [1]. The UOTCS responses are similar to those of the first model except that now the responses are faster with reduced peak overshoot (dotted curves of figure (13)). This is attributed to the reduced mass inertias. The steady state error shown in figure (15) is eliminated if a PID pitch controller is used, as shown in figure (16).

The numerical tests lead to the same result that the FLC is superior in terms of robustness and speed of response. In conclusion, the FLC is better with regard of peak overshoot and settling time when compared with the PID controller.

4. 3D Animation of UOTCS Helicopter

A 3D UOTCS Helicopter scene was created using VRML to provide a powerful tool to facilitate teaching and research (figure (17)). VRML is a scene description language which is human readable [8]. The VRML scene graph is composed of a hierarchy of nodes and routes. The UOTCS helicopter scene has three degrees of freedom. “Transform” nodes are used to control rotational values of the entire “children” nodes below it. The “children” node contains one or more objects. Each “Transform” node are named as travel, elevation and pitch, so that they can be rotated separately. Also three viewpoints and Background nodes are used to enable the UOTCS helicopter object to be viewed in different directions [6].

Using the simulink of figure (3b), the response of the helicopter over time is made visually realistic with user interaction option. Simulink provides connection for control and manipulation of virtual reality object, using virtual reality toolbox [9]. The VR toolbox is a solution for interacting with VR models of dynamic system over time.

5. Conclusions

A mathematical model for a recently built 3DOF table top helicopter experimental setup named UOTCS helicopter was successfully developed. It takes into account system nonlinearities and mass moments of inertia of the beams, the counterweight and the motors. Fuzzy logic controllers for the coupled elevation and pitch motions are successfully designed and tested. Their performance is found to be superior and robust compared with their PID controllers' counterpart. The former controllers cover a wider range of operating conditions. Finally, the developed 3D UOTCS Helicopter scene is an attractive alternative to traditional laboratory equipments which can meet educational objectives.

The theoretical model is to be extended in the future to take into account structural flexibility and propeller air friction and inertia. Also, other controller designs are to be investigated. The use of virtual reality is very useful in helping users to interact with the model and view the behavior of the UOTCS helicopter and its response over time. The overall student reaction should also be investigated and their feedback should be analyzed with the ultimate goal of providing laboratories suitable for distance learning.

6. References

[1] R. S. Abedulwahab, "Design of 3DOF Helicopter Propeller Tabletop Experimental Setup", Dept. of Control and Systems Eng., UOT, M.Sc. thesis, Baghdad, Iraq, 2006.

[2] M. Gafvert, "Modeling of ETH Helicopter Laboratory Process", Department of Automatic Control, Lund Institute of Technology, Technical Report, Seweden, November, 2001.

[3] M. A. Ishutkina, "Design and Implementation of a Supervisory Safety Controller for a 3DOF Helicopter", Massachusetts Institute of Technology, M.Sc. thesis, 15, June, 2004.

[4] M. W. Spong, Seth Hutchinson and M. Vidasayar, "Robot Modeling and Control", First edition, John Wiley & Sons Inc, USA, 2006.

[5] A. J. Koivo, "Fundamental for Control of Robotic Manipulators", First edition, John Wiley & Sons Inc, USA, 1989.

[6] M. F. Shaker, "Dynamic Control simulation of the UOTCS Helicopter Body", Dept. of Control and Systems Eng., UOT, M.Sc. thesis, Baghdad, Iraq, 2008.

[7] K. M. Passino and S. Yurkovich, "Fuzzy Control", First edition, Addition Wesley Longman Inc, USA, 1998.

[8] R. Gary, "The Virtual Reality Modeling Language Explained", Multimedia, IEEE, Vol.5, Issue 3, USA, July-Sept, 1998, pp. 84-93.

[9] Y. Zhong, "A Model Representation for Solid Modeling in a Virtual Reality Environment", Proceedings of The shape modeling International, USA, 17-22, May, 2002, pp. 183-190.

List of Symbols

C_{ijk} Christoffel's symbols.

$\boldsymbol{C}(\boldsymbol{q},\dot{\boldsymbol{q}})$ The second matrix of the Euler-Lagrange equation.

C_{ij} Elements of the matrix $\boldsymbol{C}(\boldsymbol{q},\dot{\boldsymbol{q}})$.

$\boldsymbol{D}(\boldsymbol{q})$ Inertia matrix.

d_i Offset of the frame i.

$\boldsymbol{F}$ The external generalized force vector.

F_b Back motor thrust force.

F_f Front motor thrust force.

k_d Derivative gain.

$\boldsymbol{g}(\boldsymbol{q})$ Gravitational matrix .

$\boldsymbol{J}$ Jacobian matrix.

k_{e1} Gain of the error input to elevation controller.

k_{e2} Gain of the change of error input to elevation controller.
k_{oe} Gain of the output from elevation controller.
k_{p1} Gain of error input to pitch controller.
k_{p2} Gain of the change of error input to pitch controller.
k_{op} Gain of the output from pitch controller.
$\boldsymbol{q}$ The set of the generalized coordinate for the system.
$\boldsymbol{Q}$ The vector of the generalized forces acting on the system.
$\boldsymbol{T}_i$ The homogeneous transformation related two coordinate frames (i) and (i-1) attached to the links which are connected to the rotational joint.
α_i Twist angle of the frame *i*.
ε Elevation angle.
θ Pitch angle.
θ_i Angle of the frame *i*.
$\boldsymbol{\tau}$ Travel angle.
$\boldsymbol{\tau}(\boldsymbol{q})$ Torque vector.
Note: Refer to figure (3a) for definitions of Masses (m), Lengths (L) & Inertias (I).

Table (1) Structural Kinematics Parameters

Link	Name	a_i	α_i	d_i	θ_i	θ_i - name
1	Travel joint	0	$\pi/2$	0	λ	travel
2	Elevation joint	0	$\pi/2$	0	$\varepsilon+\pi/2$	Elevation
3	Elevation joint	0	$\pi/2$	L_C*	$\varepsilon+\pi/2$	Elevation
4	Arm	-h	0	L_{af}	θ	Pitch
5	Front Motor	L_h	$\pi/2$	0	$\pi/2$	Fixed
6	Back Motor	$-L_h$	$\pi/2$	0	$\pi/2$	Fixed
7	Counter-weight	L_w	$\pi/2$	0	$\varepsilon+\pi$	Elevation

* Where $L_c = (L_{af} + L_{ae})/2$

Table (2) Elevation and Pitch Transfer Function for each Operating Point.

$[\lambda \quad \varepsilon \quad \theta]$ $[F_f \; F_b]$	[0° -30° 0°] [0 0]	[0° -30° 0°] [0.001 0.001]	[0° -15° 0°] [0 0]	[0° -15° 0°] [0.001 0.001]	[0° 0° 0°] [0.0450.0457]
Elevation T.F	$\frac{2.56}{(2.56S^2+1)}$	$\frac{2.1}{(2.08S^2+1)}$	$\frac{2.85}{(2.85S^2+1)}$	$\frac{2.5}{(2.5S^2+1)}$	$\frac{2.95}{(2.22S^2+1)}$
Pitch T.F	$\frac{1}{(0.18S^2+1)}$	$\frac{1.01}{(0.19S^2+1)}$	$\frac{0.9}{(0.17S^2+51)}$	$\frac{0.91}{(0.17S^2+1)}$	$\frac{0.87}{(0.16S^2+1)}$

Table (3) Rule-Base for Elevation and Pitch Controller.

Output		$\dot{e}$						
		NB	**NM**	**NS**	**ZR**	**PS**	**PM**	**PB**
e	**NB**	**ZR**	**NS**	**NS**	**ZR**	**PS**	**PM**	**PM**
	NM	**NM**	**ZR**	**NS**	**NS**	**PS**	**PS**	**PM**
	NS	**NM**	**NM**	**ZR**	**NS**	**PS**	**PS**	**PS**
	ZR	**NS**	**NS**	**NS**	**none**	**PS**	**PS**	**PS**
	PS	**NB**	**NM**	**NM**	**PS**	**ZR**	**PB**	**PS**
	PM	**NB**	**NM**	**ZR**	**ZR**	**PB**	**ZR**	**PB**
	PB	**NB**	**NB**	**ZR**	**ZR**	**PB**	**PB**	**ZR**

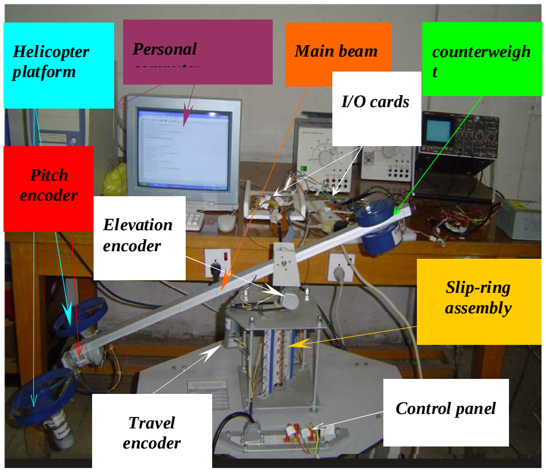

Figure (1) 3DOF UOTCS Helicopter simulator [1].

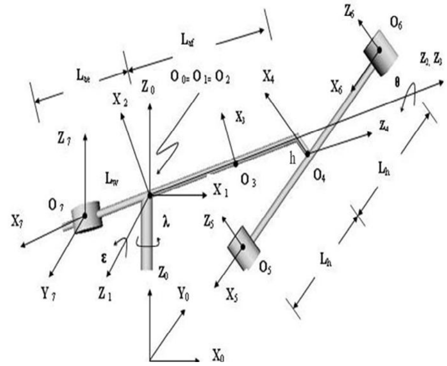

Figure (2) UOTCS Helicopter coordinates system assignment.

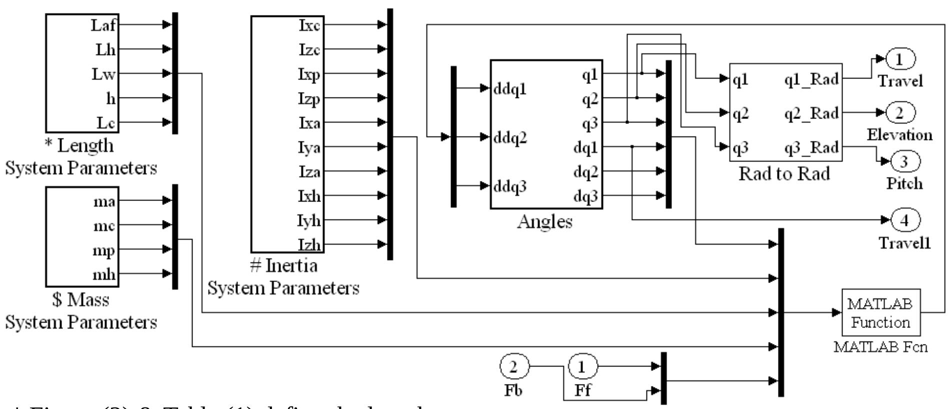

* Figure (2) & Table (1) define the lengths.
# I is the mass moment of inertia & first suffix specifies the axis, second suffix specifies: h=helicopter body, a= main beam, c=counter weight, p=front & back motor.
$ m mass & the suffix designation is as the second suffices defined in # above.

(a)

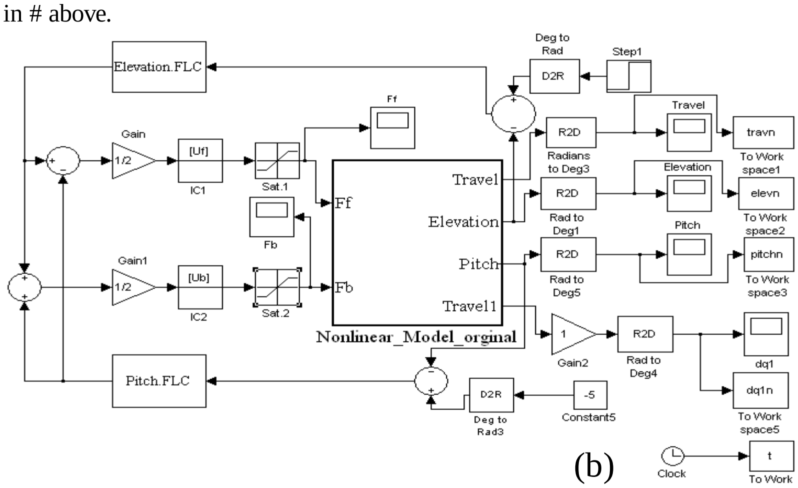

(b)

Figure (3) a) MATLAB Fnc dedicated to solve the UOTCS nonlinear differential equations. b) UOTCS nonlinear Simulink with pitch & elevation controllers [6].

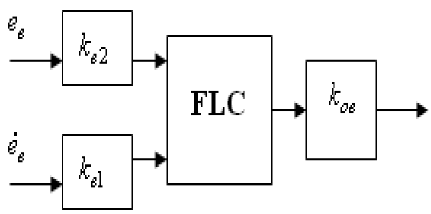

Figure (4) Elevation proportional plus integral fuzzy logic controller.

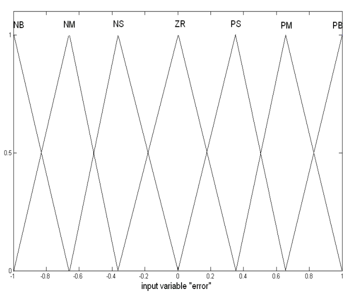

(a) Elevation controller input membership function.

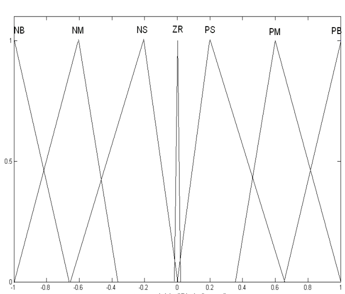

(b) Pitch controller output membership function.

Figure (5) Fuzzy sets membership function; a) Elevation controller. b) Pitch controller.

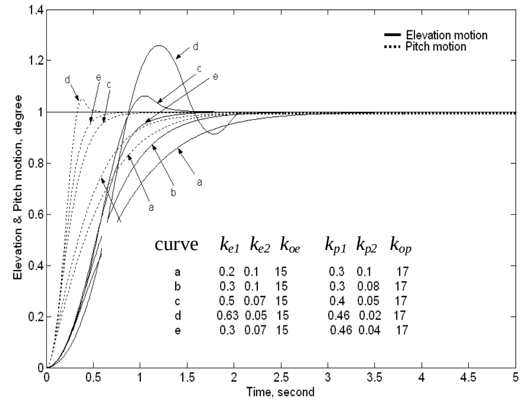

Figure (6) Step input responses when tuning FLCs with the linearized model.

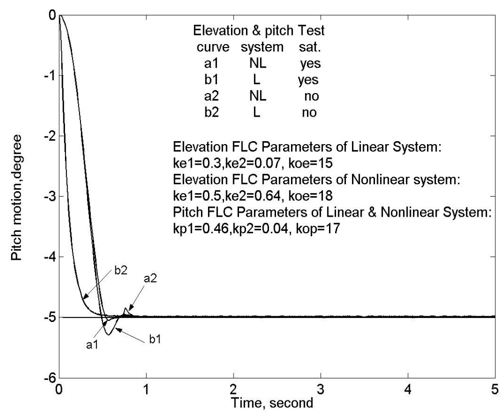

a) Pitch response (0 to -5^o).

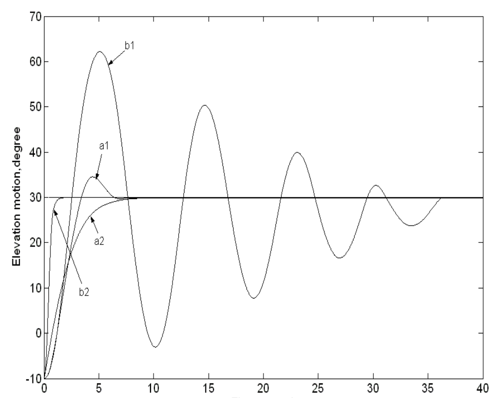

b) Elevation response (-10^o to 20^o).

Figure (7) a) Pitch & b) elevation tests Using FLC after tuning with the non-linear model.

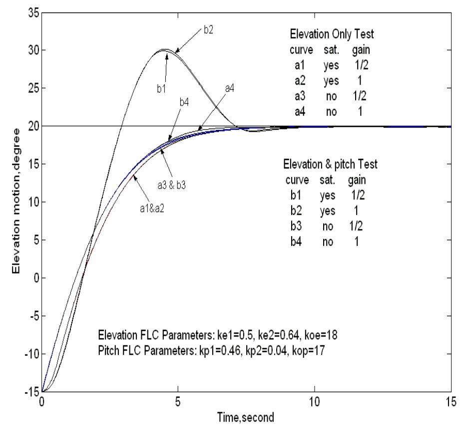

Figure (8) Elevation angle response with & without pitching of the nonlinear model.

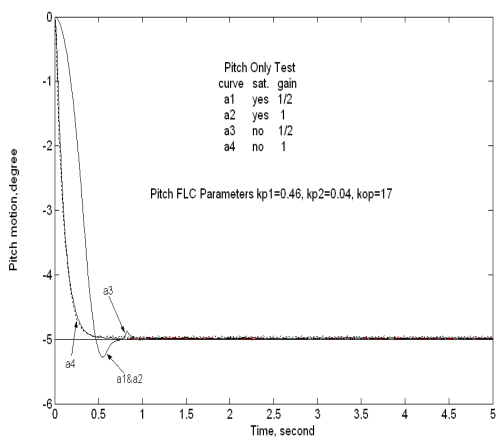

Figure (9) Pitch angle responses of the nonlinear model.

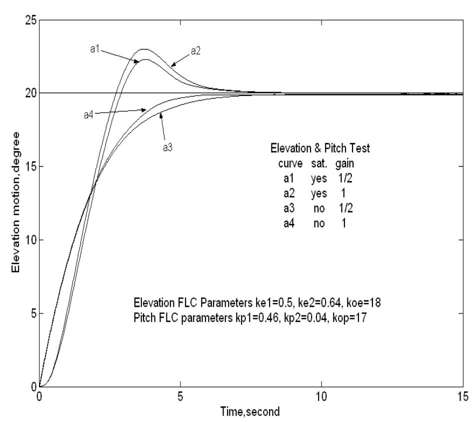

Figure (10) Elevation angle responses from level to 20^o with an initial thrust force.

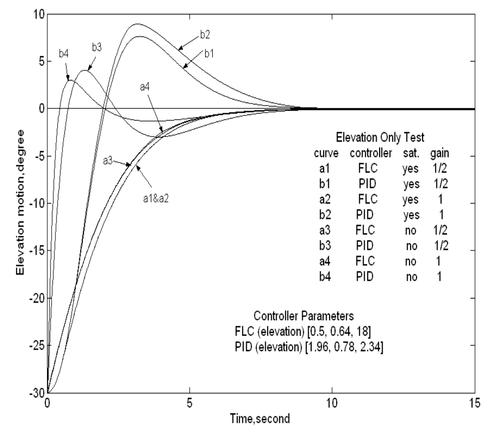

Figure (11) A comparison of elevation responses using FLC & PID controllers with & without saturation.

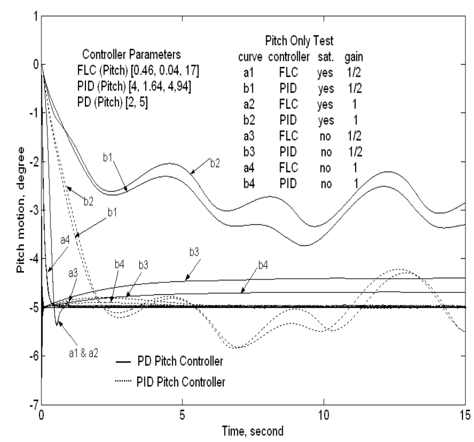

Figure (12) Performance comparison of FLC, PID & PD controllers with pitch only maneuvering.

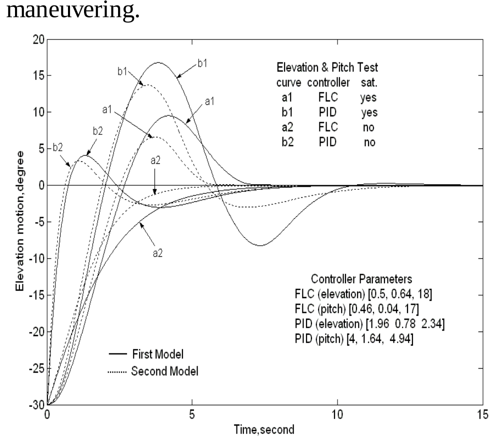

Figure (13) Elevation angle responses from -30^o to level with pitching action & usin PID pitch controller.

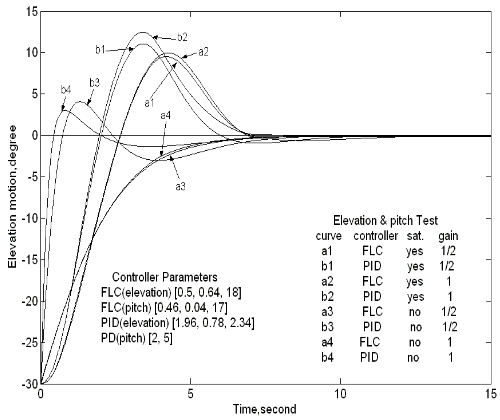

Figure (14) Elevation angle responses from -30^{o} to level with pitching action & using PD pitch controller.

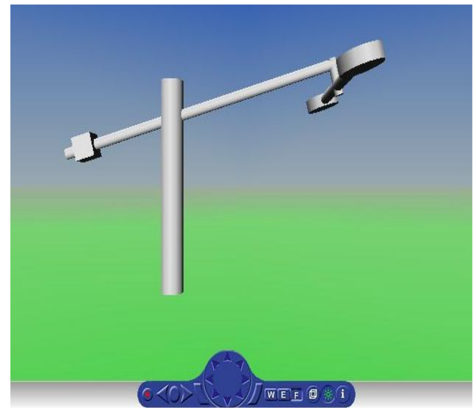

Figure (17) UOTCS helicopter scene created using VRML.

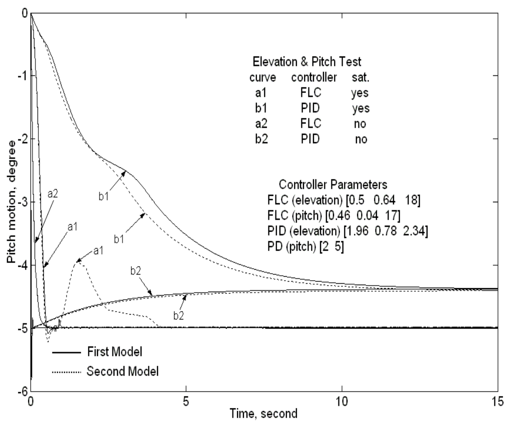

Figure (15) Pitch angle responses from 0^{o} to -5^{o} using PD pitch controller.

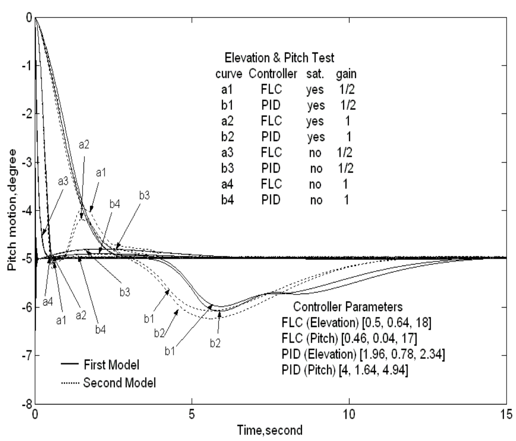

Figure (16) Pitch angle responses from 0^{o} to -5^{o} using PID pitch controller.